Direct steam generation solar systems with screw expanders and parabolic trough collectors: Energetic assessment at part-load operating conditions

Paolo Iodice [*], Giuseppe Langella, Amedeo Amoresano

Università degli Studi di Napoli Federico II, Dipartimento di Ingegneria Industriale, Italy

A B S T R A C T

This paper explains a numerical optimization of a novel screw expander-based solar thermal electricity plant to evaluate the energetic benefits in specific case studies. In the proposed solar electricity generation system, which is based on the steam Rankine cycle, water is used as working fluid and storage, parabolic trough collectors as a thermal source and screw expander as power machine. Such solar system offers major advantages over conventional power plants adopting steam turbines: low operating pressures, good exploitation of low temperature heat sources, acceptable efficiency in energy conversion with steam-liquid mixtures and reduced size. Since screw expanders can operate at off-design working conditions in several situations when installed in direct steam generation solar plants, the chief purpose of the present study is to develop a thermodynamic model to analyse the energy performance of the planned solar power system when off-design operating conditions befall. To assess maximum efficiency of the whole power plant at part-load operating conditions, numerical optimization is then performed in a specific range of fluctuating evaporation temperatures under fixed condensation pressures.

1. Introduction

Recently, much research has analyzed the advantages of renewable energy sources which have attracted increasing attention worldwide due to low temperatures, low heat values and high accessible amounts for exploitation (such as solar power and geothermal energy) [1]. In the last decades, in fact, extraordinary consumption of fossil fuels has caused many severe environmental problems all over the world, such as atmospheric pollution and global warming.

Being stimulated by such crucial questions, this paper shows a new solar electricity generation system (SEGS) with water used both as working fluid and storage. Thisparticular SEGS, which is based on a steam Rankine cycle (SRC),utilizes parabolic trough collectors (PTCs) to generate dry steam and screw expanders (SEs) to deliver mechanical power. The satisfactory applicability in energy conversion with steam–liquid mixtures makes the screw expanders suitable for exploitation of low-medium temperature heat sources. In effect, direct steam generation (DSG) power plants adopting screw expanders as power machines are at present typically used for low-grade heat recovery and low temperature applications (waste heat recovery and geothermal energy), but now these new DSG power plants can represent an actual opportunity also for use in solar electricity generation systems [2].

In general, volumetric expanders are mainly appropriate for small scale applications characterized by low flow rates for high

---

* Corresponding author. Via Claudio 21, 80125, Napoli, Italy.
E-mail address: paolo.iodice@unina.it (P. Iodice).

pressure ratios and low rotational speed, also accepting fluid in two-phase conditions [3,4]. In comparison with other volumetric power machines, SEs offer advantages of simple construction, two-phase tolerance and satisfying efficiency under low working pressure [5]. Screw expander technology delivers some advantages also in comparison with steam turbines used in large-scale SEGSs. Indeed, SEs are power machines which can be adopted to convert thermal energy to mechanical power with low net power but without reducing the steam Rankine cycle efficiency (also while expanding liquid-steam blends) [6], whereas dynamic expanders are usually utilised in existing DSG solar systems providing higher power output but without admitting two-phase flows [7,8]. The fluid velocities within steam turbines, in fact, are approximately one order of magnitude higher than those in screw expanders; thus, the risk of damage resulting from the admission of liquid/steam mixtures is very higher for turbo expanders. Taking all these features into account, screw expanders become a realistic choice for DSG solar systems with respect to both steam turbines and other sorts of volumetric machines [9–11].

In effect, the SE built-in pressure ratio can be much lower than the real working pressure ratio in most cases of (PTC)-based power plants with direct steam generation [1]. Consequently, under such operating conditions, the accessible enthalpy of high-temperature dry steam cannot be completely exploited when a single screw expander is used [12,13]. In order to produce mechanical power with acceptable efficiency even under these off-design working conditions, this study adopts a plant solution based on two screw expanders joined in series in a DSG solar system [1].

The chief purpose of the present study is to explain a thermodynamic model of the whole power plant to explore the energy assessment of SE-based DSG solar plants in specific case studies. By adopting this mathematical model at part-load working conditions, numerical optimization of all variables is developed in order to attain maximum efficiency of the proposed solar power system. The first aim of this study is to develop a mathematical model to describe the polytropic expansion phase in the SE. Subsequently, basic principles are established to assess the energy performance of this SE-based DSG solar plant. In the numerical simulations used for this SE-based DSG solar system, the evaporation temperature of water is optimized with respect to solar thermal power generation efficiency. Thus, in the typical solar radiation range between 900 W/m^2 and 300 W/m^2, numerical optimization is performed supposing evaporation temperatures progressively increasing from 170 °C to 320 °C, under condensation pressures of water assumed equal to 0.1 bar and 1 bar.

2. Mathematical models

Solar systems which employ parabolic trough collectors represent an encouraging technology; in effect, the worldwide capacity of these solar plants represents nearly 95% of actual solar power systems [14–16]. Furthermore, in the field of real SEGS, power systems with direct steam generation based on parabolic trough collectors represent a hopeful technology also for cost reduction [17,18].

The solar power collector efficiency η_{PTC} of a parabolic trough collector (sole module) is evaluated by Equation (1), where T_a (K) is ambient temperature, T (K) is temperature at the PTC inlet and G_b (W/m^2) is beam solar radiation [5,12,13]:

$$\eta_{PTC}(T) = 0.762 - 0.2125 \cdot \frac{T - T_a}{G_b} - 0.001672 \cdot \frac{(T - T_a)^2}{G_b} \tag{1}$$

In (PTC)-based power plants with DSG, water in parabolic trough collectors is both in binary phase and liquid phase regions. In liquid phase region, to obtain an outlet temperature T_{out} with a specific inlet temperature T_{in}, the necessary collector area A_l can be evaluated as in Equation (2), where the solar energy collection efficiency η_{PTC} is estimated with Eq. (1), $\dot{m}$ is the mass flow rate of water through the PTC and $C_p(T)$ is the heat capacity of water that can be calculated in Equation (3) by a first order approximation (T is the temperature of water in the liquid phase region ranging between T_{in} and T_{out}) [1].

$$A_l = \int_{T_{in}}^{T_{out}} \frac{\dot{m} \cdot C_p(T)}{\eta_{PTC}(T) \cdot G_b} dT \tag{2}$$

$$C_p(T) = C_{p,0} + \alpha(T - T_0) \tag{3}$$

Clearly, the solar energy collection efficiency $\eta_{PTC,b}$ in binary phase region can be estimated with Eq. (1) because water temperature remains constant in this phase. Consequently, in the binary phase region, the necessary collector area A_b can be calculated by Equation (4), in which Δh_b is the enthalpy increase of water [6]:

$$A_b = \frac{\dot{m} \cdot \Delta h_b}{\eta_{PTC,b} \cdot G_b} \tag{4}$$

For DSG power plants, as the solar field consists of liquid-steam mixture, the overall solar power collector efficiency can be assessed as in Equation (5), where $\dot{Q}$ represents the heat global transfer rate of water, A is the PTC global collector area (that is the sum of elementary modules), and h_2 and h_3 are the enthalpies of water at the PTC inlet and PTC outlet, respectively [19,20].

$$\eta_{PTC}(T) = \frac{\dot{Q}}{G_b \cdot (A_l + A_b)} = \frac{\dot{m} \cdot (h_3 - h_2)}{G_b \cdot A} \tag{5}$$

The screw expander is a rotary-type positive displacement machine that can produce mechanical energy without high working fluid velocities, by using enthalpy in working fluid characterized by high temperature and pressure [21,22]. Thus, screw expanders offer many advantages compared to dynamic expanders; indeed, these volumetric machines show good acceptance of steam-liquid

mixtures, from superheated steam to saturated liquid [23,24].

The polytropic and isentropic expansion processes are shown in the *p-V* diagrams of Fig. 1. In ideal isentropic conditions, the expansion process of the working fluid follows the path A-3-4_b-B. However, since there are some energy losses which characterize screw expanders in real working situations (so reducing the ideal work output) [25,26], the following four efficiencies can be introduced [1,12]:

- η_{Th} is the theoretical efficiency which contemplates losses owing to ill-matching of the real pressure ratio $r_p = p_3/p_4$ to the built-in pressure ratio $r_{p,b} = p_3/p_{4b}$ [2];
- η_L considers fluid leakage losses between the rotating helical screws;
- η_{ti} is the thermodynamic efficiency which considers energy losses due to thermodynamic irreversibility;
- η_m is the mechanical efficiency which represents mechanical losses owing to frictions from the moving rotors in the SE.

In Equation (6), the SE overall isentropic efficiency η_{SE} contemplates all the efficiencies itemized above [5,8], with $\eta_D = \eta_L \cdot \eta_{ti}$ that is defined as the diagram efficiency. Hence, the influence of energy losses due to thermodynamic irreversibility on the overall screw expander efficiency η_{SE} are included in the diagram efficiency η_D.

$$\eta_{SE} = \eta_{Th} \cdot \eta_L \cdot \eta_{ti} \cdot \eta_m = \eta_{Th} \cdot \eta_D \cdot \eta_m \qquad (6)$$

All these energy losses can be evaluated by noticing the state points shown in Fig. 1. Losses during admission phase are represented in the path from A to $3'$ (in blue line) while losses during discharge phases are represented in the paths from $5'$ to B' and from $5''$ to B'' (in blue lines). Energy losses due to thermodynamic irreversibility are represented in the expansion process from $3'$ to $4'$. Obviously, in real operating situations, these paths (in blue lines) follow equation $P \cdot v^n = const$, in which the polytropic index n replaces the index k of an ideal isentropic case to give the real expansion path of working fluid when it is correlated against the specified inlet and outlet conditions [6,12].

Lastly, Fig. 1 also shows energy losses due to ill-matching of the SE built-in discharge pressure (that is equal to p_{4b} in ideal isentropic case and $p_{4'}$ in polytropic expansion process) to the operating discharge pressure p_4 (real exhaust pressure ranging between $p_{B'}$ and $p_{B''}$), that cause either a blowdown effect (patch from $4'$ to $5'$ in Fig. 1 (I)) or a blowback effect (patch from $4'$ to $5''$ in Fig. 1 (II)). In this regard, a chief characteristic of screw expanders is a small built-in volume ratio $r_{v,b} = v_{4,b}/v_3$. Generally, since a small built-in volume ratio is required to exploit the mass flow rate of working fluid before the high pressure port is closed, this parameter usually ranges between 3 and 6 [12]. However, an excessively low built-in volume ratio means a small built-in expansion ratio ($r_{p,b} = r_{v,b}^k$), thereby causing under-expansion conditions when the actual pressure ratio r_p in real power systems exceeds the built-in expansion ratio $r_{p,b}$. Under such operating condition, the working fluid is exhausted at too high a pressure, thereby reducing the available energy and involving off-design operating conditions of the SE [1].

In the isentropic expansion phase, the specific ideal work produced by a steady-flow screw expander can be evaluated by the area undergoing the ideal diagram $P \cdot v^k = const$ (shown in the path from 3 to 4_b in Fig. 1). This ideal work is calculated as in Equation (7) and can be called theoretical isentropic work W_{Ti} [1,12].
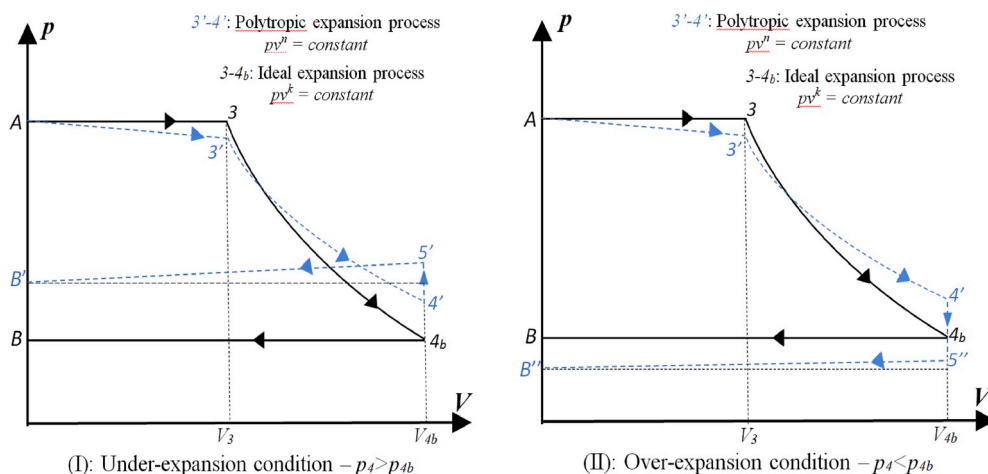

Fig. 1. (I): Polytropic expansion process with a blowdown effect during under-expansion conditions (patch in blue line: A-$3'$-$4'$-$5'$-B') and isentropic expansion process (path A-3-4_b-B), (II): Polytropic expansion process with a blowback effect during over-expansion conditions (patch in blue line: A-$3'$-$4'$-$5''$-B'') and isentropic expansion process (path A-3-4_b-B). (For interpretation of the references to colour in this figure legend, the reader is referred to the Web version of this article.)

$$W_{Ti} = -\int_3^{4b} v\,dp = -\int_3^{4b}[d(pv) - p\,dv] = p_3 v_3 - p_{4b}v_{4b} + \int_3^{4b} p\,dv = \frac{k}{k-1}p_3 v_3\left(1 - r_p^{\frac{1-k}{k}}\right) \tag{7}$$

In Equation (8), the theoretical efficiency η_{Th} is obtained by dividing the theoretical diagram work W_{Td} (that is the net work obtained when the real discharge pressure p_4 differs from the SE built-in expansion pressure p_{4b} relevant to an isentropic case) by the theoretical isentropic work W_{Ti} expressed in Equation (7). Hence η_{Th} represents losses owing to ill-matched real expansion ratio r_p and built-in expansion ratio $r_{p,b}$.

$$\eta_{Th} = \frac{W_{Td}}{W_{Ti}} = \frac{\frac{1}{k-1}p_3 v_3\left(1 - r_{p,b}^{\frac{1-k}{k}}\right) + p_3 v_3\left(1 - \frac{r_{p,b}^{\frac{k}{k}}}{r_p}\right)}{\frac{k}{k-1}p_3 v_3\left(1 - r_p^{\frac{1-k}{k}}\right)} = \frac{\left(1 - r_{v,b}^{1-k}\right) + (k-1)\left(1 - \frac{r_{v,b}}{r_p}\right)}{k\left(1 - r_p^{\frac{1-k}{k}}\right)} \tag{8}$$

In Equation (9) the diagram efficiency η_D is obtained by dividing the thermodynamic work W_{Tm} (that is the sum of the shaft work output W_S and the work for mechanical frictions W_{MF}) by the theoretical diagram work W_{Td}. Thus, this efficiency η_D contemplates losses due to both thermodynamic irreversibility and fluid leakage losses (during discharge and admission phases) [1]. In a previous scientific publication [23], the variation in diagram efficiency η_D with r_p and $r_{v,b}$ was exposed when saturated vapour is used as working fluid. It was shown that the diagram efficiency η_D can be reduced by high built-in volume ratio $r_{v,b}$, but the relevant reductions become insignificant under rising real pressure ratios r_p. In effect, when the operating expansion ratios are almost twice the built-in expansion ratio $r_{p,b}$, the values of the diagram efficiency become around constant with the operating pressure ratio r_p.

$$\eta_D = \frac{W_{Tm}}{W_{Td}} = \frac{W_S + W_{MF}}{p_3 v_3\left[\left(\frac{1 - r_{v,b}^{1-k}}{k-1}\right) + \left(1 - \frac{r_{v,b}}{r_p}\right)\right]} \tag{9}$$

When the theoretical efficiency η_{Th} reaches its maximum $\eta_{Th,p}$, the isentropic efficiency η_{SE} reaches its peak value $\eta_{SE,p}$, as shown in Equation (10). With the assumption of the maximum theoretical efficiency $\eta_{Th,p}$ as unitary, the overall isentropic efficiency of the screw expander can be calculated as in Equation (11) [1]. Thus, the peak isentropic efficiency $\eta_{SE,p}$ comprises fluid leakage losses, losses due to mechanical frictions and energy losses due to thermodynamic irreversibility. Finally, as explained in Equation (11), once the built-in volume ratio $r_{v,b}$, the isentropic index k and the peak isentropic efficiency $\eta_{SE,p}$ are fixed, the overall isentropic efficiency η_{SE} depends on the operating pressure ratio r_p.

$$\eta_{SE,p} = \eta_{Th,p}\cdot\eta_L\cdot\eta_{ti}\cdot\eta_m = \eta_{Th,p}\cdot\eta_D\cdot\eta_m \tag{10}$$

$$\eta_{SE} = \eta_{SE,p}\cdot\eta_{Th} = \eta_{SE,p}\cdot\frac{\left(1 - r_{v,b}^{1-k}\right) + (k-1)\left(1 - \frac{r_{v,b}}{r_p}\right)}{k\left(1 - r_p^{\frac{1-k}{k}}\right)} \tag{11}$$

Equation (12) shows the steam Rankine cycle efficiency η_{SRC}, where P_{SRC} is the power of the Rankine cycle (difference between the SE power P_{SE} and the power absorbed by the pump P_p) and $\dot{Q}$ is the heat transfer rate of water in the binary phase and liquid phase regions [1,19]. In such equation, η_{SE} is the global efficiency of the screw expander (already shown in Equation (11)), h_1 is the enthalpy value of water at the pump inlet, η_p is the pump overall efficiency which considers both the adiabatic and mechanical efficiency of the pump and $h_{2,is}$ is the isentropic enthalpy at the pump outlet, which can be calculated on the basis of water enthalpy properties by using REFPROP tables once the pressure increase is fixed. Besides, h_3 is the enthalpy value at the SE inlet and $h_{4,is}$ is the isentropic enthalpy value at the SE outlet. Clearly, all these enthalpy values depend on the specific steam Rankine cycle.

$$\eta_{SRC} = \frac{P_{SRC}}{\dot{Q}} = \frac{P_{SE} - P_P}{\dot{Q}} = \frac{(h_3 - h_{4,is})\cdot\eta_{SE} - (h_{2,is} - h_1)/\eta_p}{(h_3 - h_2)} \tag{12}$$

In Equation (13) and Equation (14), η_G is the solar thermal power efficiency which describes the share of solar radiation efficiently converted into output power $P_{NET} = P_{SRC}\cdot\eta_{mec}$ (net power produced by the PTC-based power system), where η_{mec} is the mechanical efficiency of the PTC-based power system (also comprising generator efficiency) [12]. Therefore, this overall efficiency can be considered the global efficiency of the DSG power system as a whole.

$$\eta_G = \frac{P_{NET}}{G_b\cdot A} = \eta_{PTC}\cdot\eta_{SRC}\cdot\eta_{mec} \tag{13}$$

$$\eta_G = \eta_{PTC} \left[\frac{(h_3 - h_{4,is}) \cdot \eta_{SE,p} \cdot \dfrac{\left(1 - r_{v,b}^{1-k}\right) + (k-1)\left(1 - \dfrac{r_{v,b}}{r_p}\right)}{k\left(1 - r_p^{\frac{1-k}{k}}\right)} - \dfrac{(h_{2,is} - h_1)}{\eta_p}}{(h_3 - h_2)} \right] \eta_{mec} \tag{14}$$

3. Results and discussion

The particular SE-based DSG solar plant examined in this paper is presented in Fig. 2, whereas the *T-s* diagram of the steam Rankine cycle is shown in Fig. 3 under evaporation temperature and condensation pressure assumed equal to 200 °C and 1 bar, respectively [12]. As shown in the schematic diagram, the saturated steam flows into two screw expanders in tandem configuration to deliver mechanical energy. The expansion phase starts in the first screw expander SE_1 (path from *3* to *3'*) and it is then concluded in the second screw expander, SE_2 (path from *3'* to *4*). Thus, the exhausted steam flows into condenser C (path from *4* to *1*) to be condensed. Lastly, the saturated liquid is pressurized by pump P_1 (patch from *1* to *2*) in the direction of the parabolic trough collectors (*PTCs*) to generate saturated steam, which is finally separated in the steam separator unit (SS), so producing dry saturated steam [1].

In the mathematical simulations adopted for this steam Rankine cycle, two SEs are coupled in series in order to decrease the actual expansion ratio r_p of each screw expander. Indeed, as was clarified in the previous section, SE isentropic efficiency decreases when the real expansion ratio r_p increases excessively in comparison with the SE built-in expansion ratio $r_{p,b}$, thus involving off-design operating conditions [6]. Consequently, by adopting such a plant configuration, the entire expansion ratio is shared on two screw expanders, such that each power machine can profit from lower real expansion ratio r_p.

Numerical optimization of this sort of SE-based DSG solar plant is improved by linking algorithms established for the energetic assessment of the whole power plant with thermodynamic formulas obtained for the SE part-load behavior [1]. In order to derive maximum solar thermal power efficiency for solar radiation G_b ranging between 900 W/m^2 and 300 W/m^2, numerical optimization considered specific case studies; condensation pressure p_4 is assumed equal to 0.1 bar and 1 bar and evaporation temperature T_3 of water (at the SE_1 inlet) is assumed to be fluctuating between 170 °C to 320 °C. By applying this mathematical model and fixing all main factors for numerical simulations (as reported in Table 1), the evaporation temperatures can be optimized with respect to steam Rankine cycle efficiency and solar thermal power generation efficiency for the fixed condensation pressures.

Using Equation (1), in Fig. 4 variations in the solar power collection efficiency with evaporation temperature are shown in the specified solar radiation range. It is obvious that the heat collector efficiency η_{PTC} always declines with evaporation temperature T_3 [1, 12].

Assuming Equation (11) (which exposes variations in SE isentropic efficiency η_{SE} with the operating pressure ratio r_p), in Fig. 5, η_{SE} is calculated against vaporization temperature T_3 when condensation pressure p_4 is supposed equal to 0.1 bar and 1 bar, once the built-in volume ratio $r_{v,b}$ is set.

For the PTC-SRC power plant proposed in this paper, on analyzing in Fig. 5 the over-expansion working conditions ($r_p > r_{p,b}$), a
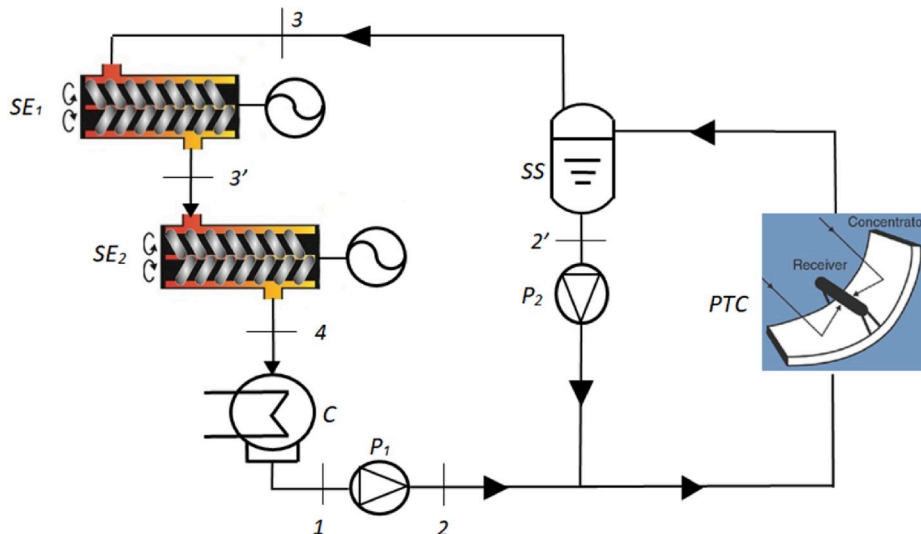

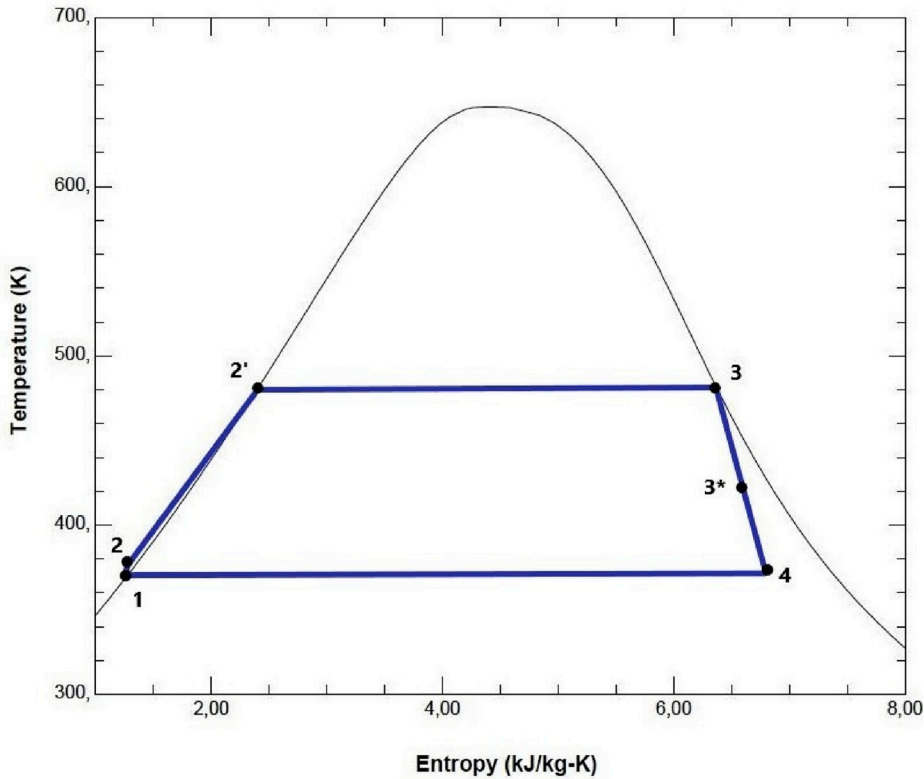**Fig. 2.** Plant configuration of the PTC-SRC power system.

Fig. 3. T-s diagram cycle of the steam Rankine cycle when T_3 is 200 °C and p_4 is 1 bar [12].

Table 1
Set parameters.

Terms	Value
T_a [C°]: ambient temperature	25
η_{mec}: mechanical efficiency	0.95
η_p: pump efficiency	0.80
k: isentropic index	1.13
$r_{v,b}$: SE built-in volume ratio	5
$\eta_{SE,p}$: SE peak isentropic efficiency	0.75

decrease in SE efficiency η_{SE} is manifest when actual condensation pressure drops from 1 bar to 0.1 bar. In effect, with rising evaporation temperature T_3 and decreasing exhaust pressure p_4, the resultant actual expansion ratio r_p increases gradually (compared to the built-in pressure ratio), hence causing off-design working conditions (blowback effect) [12]. Moreover, in Fig. 5, similar decreases in the SE overall efficiency η_{SE} are also manifest when $r_p < r_{p,b}$, namely in under-expansion operating conditions. In fact, in this other case (when exhaust pressure p_4 is assumed equal to 1 bar and evaporation temperature T_3 drops), the resultant actual pressure ratio r_p becomes progressively lower than the built-in expansion ratio, thereby causing blowdown operating conditions [5]. In effect, the maximum SE isentropic efficiency falls when the real expansion ratios r_p of both screw expanders reach the built-in expansion ratio $r_{p,b}$, whereas the mismatch of the working expansion ratio r_p with the built-in expansion ratio involves two opposite conditions: a blowback effect during the over-expansion process and a blowdown effect during the under-expansion process [1].

Using equation (12), η_{SRC} (steam Rankine cycle efficiency) results from SE isentropic efficiency η_{SE} and real pressure ratio r_p. In Fig. 6, this heat-to-power conversion efficiency is shown against evaporation temperature under condensation pressure assumed equal to 0.1 bar and 1 bar. For low evaporation temperature and high condensation pressure, the steam Rankine cycle efficiency is clearly damaged both by a decrease in the available enthalpy of expansion and a decrease in SE isentropic efficiency η_{SE} due to extreme under-expansion conditions (the resultant real pressure ratio r_p decreases overall in comparison with the SE built-in expansion ratio, thereby causing the blowdown effect which induces poor SE performance) [1].

By contrast, steam Rankine cycle efficiency always increases with rising temperature T_3 when condensation pressure p_4 is assumed equal to 1 bar. Consequently, under such working conditions, a rise in the obtainable enthalpy of expansion with a rising evaporation temperature overcomes a reduction in overall efficiency of the screw expanders (due to under-expansion conditions). However, when
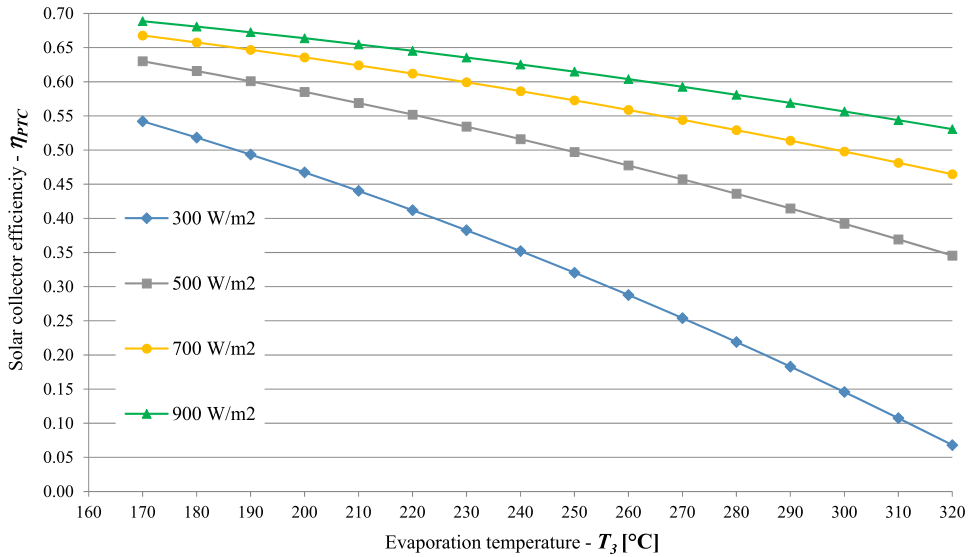
Fig. 4. Heat collection efficiency η_{PTC} with evaporation temperature under increasing solar radiation.
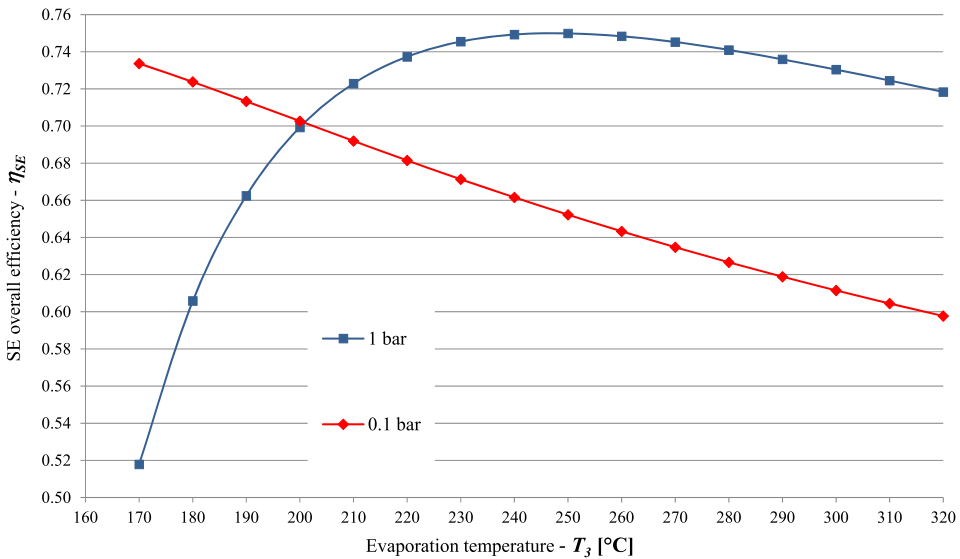

Fig. 5. Variations in SE overall efficiency with evaporation temperature under condensation pressure assumed equal to 0.1 bar and 1 bar.

condensation pressure p_4 is assumed equal to 0.1 bar, efficiency η_{SRC} becomes almost constant with rising temperature T_3 because a decrease in SE overall efficiency as evaporation temperature increases equipoises a rise in the available enthalpy of expansion [1]. Indeed, in this specific case, the heat-to-power conversion efficiency is damaged by extreme over-expansion conditions due to the blowback effect [12].

For the DSG power plant proposed in this study, by adopting Equation (14), variations in solar thermal power generation efficiency with evaporation temperature are calculated in Fig. 7 for condensation pressures assumed equal to 0.1 bar (red lines) and 1 bar (blu lines). As expounded in Equation (13), this overall efficiency η_G depends on heat collection efficiency η_{PTC}, heat-to-power conversion efficiency η_{SRC} and mechanical efficiency η_{mec}. Hence, once the SE built-in volume ratio is fixed as in Table 1, the global efficiency η_G is a function of evaporation temperature T_3, actual expansion ratio r_p and beam solar radiation G_b [27,28].

When condensation pressure is supposed equal to 0.1 bar, Fig. 7 reveals that low vaporization temperatures produce almost constant efficiencies η_G compared to its maximum values. However, for high vaporization temperature T_3 (then in extreme over-expansion conditions), the global efficiency η_G drops due to energy losses from the blowback effect. When the condensation pressure is supposed equal to 1 bar and under solar radiation higher than 500 W/m^2, it is clear that high temperatures T_3 involve moderately lower efficiencies η_G. On the other hand, for low vaporization temperatures T_3, the global efficiency η_G is reduced owing to
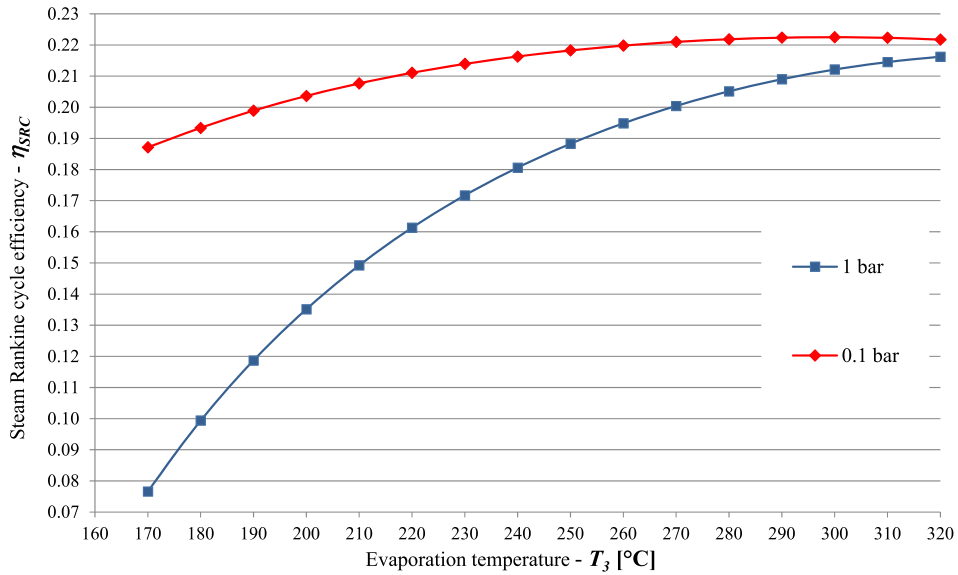
Fig. 6. Steam Rankine cycle efficiency versus evaporation temperature under condensation pressure assumed equal to 0.1 bar and 1 bar.
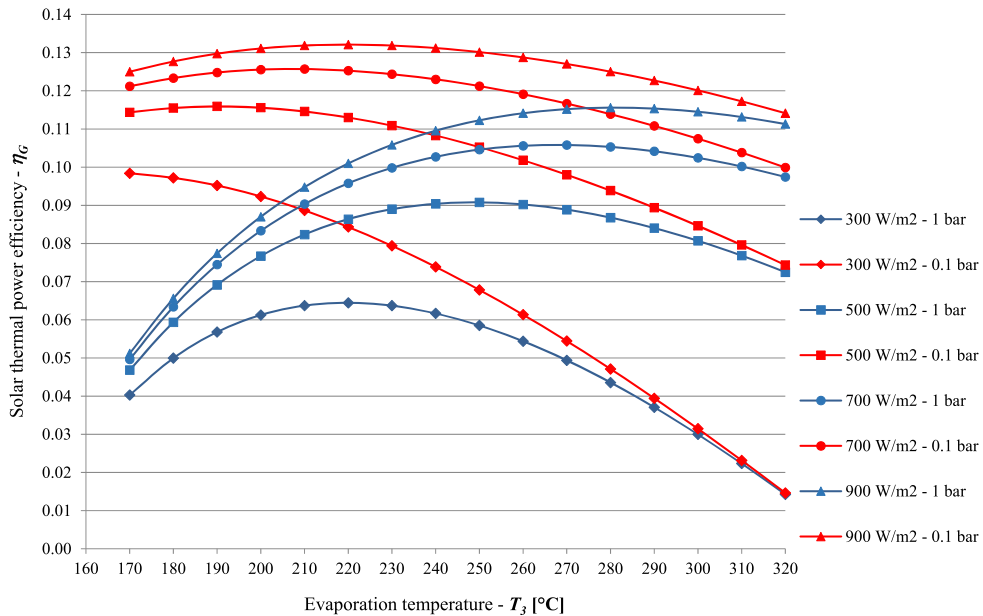

Fig. 7. Variations in global efficiency with evaporation temperature when condensation pressure is assumed equal to 1 bar and 0.1 bar under each solar radiation.

excessive under-expansion conditions that involve poor SE performance (blowdown effect) [12].

In order to discover optimum operating conditions under the fixed condensation pressures, the first derivative of each of these functions indicating variations in global efficiency η_G with solar radiation G_b and vaporization temperature T_3 were calculated and fixed to zero [1]. Using this numerical procedure, variations in the optimum vaporization temperature $T_{3,op}$ and the resulting optimum solar thermal power efficiency $\eta_{G,op}$ were found and shown in Fig. 8 and Fig. 9, respectively.

In effect, the optimum global efficiencies are attained when the condensation pressure is assumed equal to 0.1 bar, because a rise in the obtainable enthalpy of expansion with a declining condensation pressure p_4 overcomes a reduction in overall efficiency of screw expanders in over-expansion working conditions. The results displayed in Fig. 8 show that, when condensation pressure is fixed to 0.1 bar, the optimum evaporation temperature growths from around 160 °C–220 °C with rising solar radiation. Besides, on examining Fig. 9, under such specific operating condition ($p_4 = 0.1$ bar), the maximum global efficiency $\eta_{G,op}$ rises from around 10%–13% when
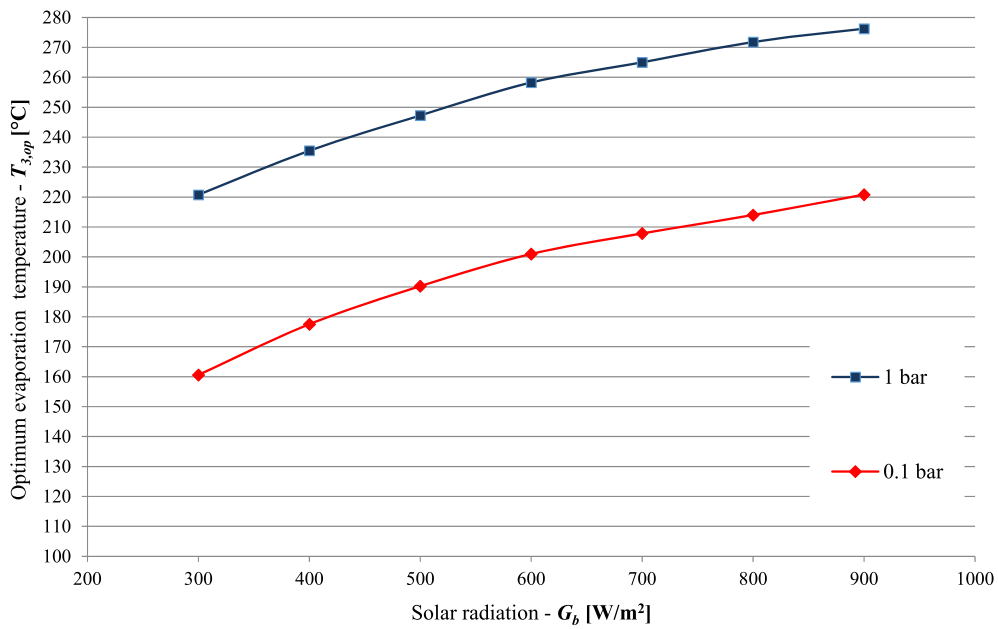
Fig. 8. Variations in optimum evaporation temperature with solar radiation when condensation pressure is assumed equal to 1 bar and 0.1 bar.
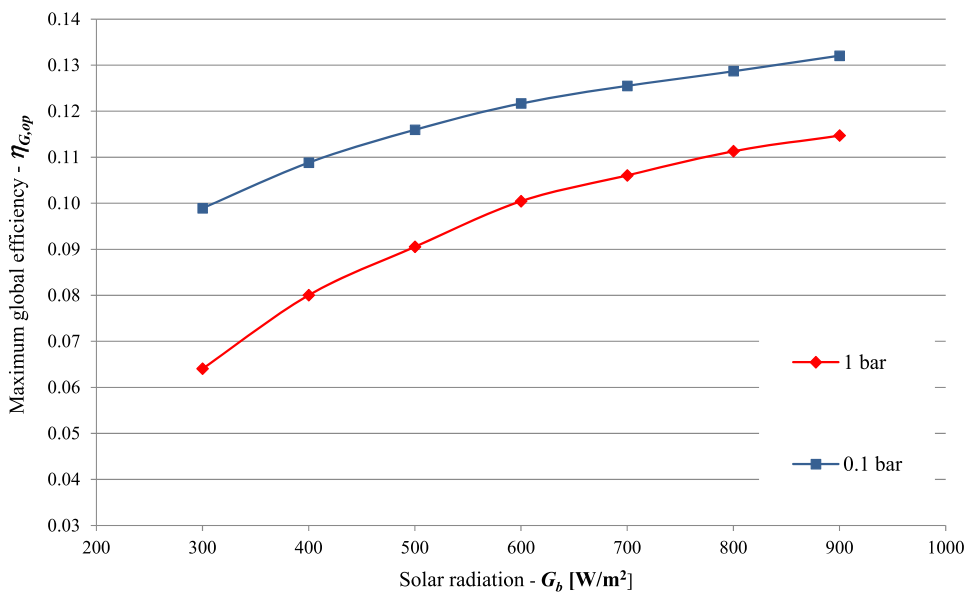

Fig. 9. Variations in optimum overall efficiency with solar radiation when condensation pressure is assumed equal to 1 bar and 0.1 bar.

solar radiation rises from 300 W/m^2 to 900 W/m^2. Therefore, this SE-based DSG solar system, in the established range of the best operating conditions, can work at lower vaporization temperatures than alike solar power plants using steam turbines, without significant reduction in global efficiency [1].

4. Conclusions

The PTC-SRC power plants based on steam SEs offer several advantages regarding the low temperature and pressure in the solar field and low technical requirements. The solar electricity generation plant analyzed in this study adopts screw expanders and parabolic trough collectors, and is based on the steam Rankine cycle. To assess best operating conditions of the proposed solar power plant at part-load working conditions and to maximize its global efficiency, numerical optimization was performed in a wide range of

variable evaporation temperatures under fixed condensation pressures.

The chief conclusions on the energy performance of this particular DSG solar power plant can be reassumed as follows:

- Under condensation pressure assumed equal to 0.1 bar, low evaporation temperatures produce a little lower or nearly constant global efficiencies in comparison with its maximum levels. Instead, for high evaporation temperatures, the global efficiency decreases owing to energy losses from the blowback effect.
- Under condensation pressure assumed equal to 1 bar and when beam solar radiation is higher than 500 W/m^2, high evaporation temperatures lead to moderately lower global efficiencies. By contrast, for low evaporation temperatures, the overall efficiency is damaged by extreme under-expansion conditions which cause reduced SE performance.
- The best global efficiencies are reached when the condensation pressure is supposed equal to 0.1 bar because a rise in the available enthalpy of expansion with a decreasing exhaust pressure overcomes a reduction in overall efficiency of screw expanders in over-expansion operating conditions. For this specific working condition, the optimum evaporation temperature is around 220 °C under higher solar radiation, with the resultant maximum global efficiency that is around 13.2%.

Declaration of competing interest

The authors state that there are not any financial and personal relationships with other people or organizations that have inappropriately influenced this paper.

CRediT authorship contribution statement

Paolo Iodice: Writing - original draft, Methodology, Formal analysis, Investigation, Software, Writing - review & editing. **Giuseppe Langella:** Conceptualization, Formal analysis, Writing - review & editing. **Amedeo Amoresano:** Conceptualization, Formal analysis, Writing - review & editing.

References

[1] P. Iodice, G. Langella, A. Amoresano, Energy performance and numerical optimization of a screw expander-based solar thermal electricity system in a wide range of fluctuating operating conditions, Int. J. Energy Res. 44 (2020) 1858–1874, https://doi.org/10.1002/er.5037.
[2] Y. Zhu, L. Jiang, V. Jin, L. Yu, Impact of built-in and actual expansion ratio difference of expander on ORC system performance, Appl. Therm. Eng. 71 (2014) 548–558.
[3] I.K. Smith, N. Stosic, A. Kovacevic, Power Recovery from Low Grade Heat by Means of Screw Expanders, Elsevier, 2014.
[4] F. Fatigati, M. Di Bartolomeo, R. Cipollone, Dual intake rotary vane expander rechnology: experimental and theoretical assesment, Energy Convers. Manag. 186 (2019) 156–167.
[5] J. Li, P. Li, G. Pei, J.Z. Alvi, J. Ji, Analysis of a novel solar electricity generation system using cascade Rankine cycle and steam screw expander, Appl. Energy 165 (2016) 627–638.
[6] J. Li, P. Li, G. Gao, G. Pei, Y. Su, J. Ji, Thermodynamic and economic investigation of a screw expander-based direct steam generation solar cascade Rankine cycle system using water as thermal storage fluid, Appl. Energy 195 (2017) 137–151.
[7] M. Read, N. Stosic, I.K. Smith, Optimization of screw expanders for power recovery from low-grade heat sources, Energy Technol. Pol. 1 (2014) 131–142.
[8] C. Invernizzi, P. Iora, P. Silva, Bottoming micro-Rankine cycles for micro-gas turbines, Appl. Therm. Eng. 27 (2007) 100–110.
[9] P. Li, J. Li, G. Gao, G. Pei, Y. Su, J. Ji, B. Ye, Modeling and optimization of solar-powered cascade Rankine cycle system with respect to the characteristics of steam screw expander, Renew. Energy 112 (2017) 398–412.
[10] I.K. Smith, N. Stosic, A. Kovacevic, Screw expanders increase output and decrease the cost of geothermal binary power plant systems, Trans. Geotherm. Resour. 29 (2005) 787–794.
[11] I. Papes, J. Degroote, J. Vierendeels, New insights in twin screw expander performance for small scale ORC systems from 3D CFD analysis, Appl. Therm. Eng. 91 (2015) 535–546.
[12] P. Iodice, G. Langella, A. Amoresano, Modeling and energetic-exergetic evaluation of a novel screw expander based direct steam generation solar system, Appl. Therm. Eng. 155 (2019) 82–95.
[13] P. Li, J. Li, R. Tan, Y. Wang, G. Pei, B. Jiang, J. Tang, Thermo-economic evaluation of an innovative direct steam generation solar power system using screw expanders in a tandem configuration, Appl. Therm. Eng. 148 (2019) 1007–1017.
[14] L. Li, J. Sun, Y. Li, Y.L. He, H. Xu, Transient characteristics of a parabolic trough direct-steam-generation process, Renew. Energy 135 (2019) 800–810.
[15] L. Li, J. Sun, Y. Li, Thermal load and bending analysis of heat collection element of direct-steam-generation parabolic-trough solar power plant, Appl. Therm. Eng. 127 (2017) 1530–1542.
[16] H. Price, E. Lupfert, D. Kearney, E. Zarza, G. Cohen, R. Gee, et al., Advances in parabolic trough solar power technology, J. Sol. Energy Eng. 124 (2002) 109–125.
[17] L. Li, Y.S. Li, J. Sun, Prospective fully-coupled multi-level analytical methodology for concentrated solar power plants: applications, Appl. Therm. Eng. 118 (2017) 159–170.
[18] L. Li, J. Sun, Y.S. Li, Prospective fully-coupled multi-level analytical methodology for concentrated solar power plants: general modelling, Appl. Therm. Eng. 118 (2017) 171–187.
[19] P. Iodice, G. Langella, A. Amoresano, Optimization of medium temperature direct steam generation solar plant, Energy Procedia 148 (2018) 122–129.
[20] D. Laing, C. Bahl, T. Bauer, D. Lehmann, W.D. Steinmann, Thermal energy storage for direct steam generation, Sol. Energy 85 (2011) 627–633.
[21] D.L. Margolis, Analytical modeling of helical screw turbines for performance prediction, ASME J. Eng. Power 100 (1978) 482–487.
[22] H. Taniguchi, K. Kudo, W.H. Giedt, I. Park, S. Kumazawa, Analytical and experimental investigation of two-phase flow screw expanders for power generation, ASME J. Eng. Gas Turbines Power 110 (1988) 628–635.
[23] K.C. Ng, T.Y. Bong, T.B. Lim, A thermodynamic model for the analysis of screw expander performance, Heat Recovery Syst. CHP 10 (1990) 119–133.
[24] W. Wang, Y.T. Wu, C.F. Ma, G.D. Xia, J.F. Wang, Experimental study on the performance of single screw expanders by gap adjustment, Energy 62 (2013) 379–384.
[25] H. Tang, H. Wu, X. Wang, Z. Xing, Performance study of a twin-screw expander used in a geothermal organic Rankine cycle power generator, Energy 90 (2015) 631–642.

[26] I.K. Smith, N. Stosic, E. Mujic, A. Kovacevic, Steam as the working fluid for power recovery from exhaust gases by means of screw expanders, Proc. Inst. Mech. Eng. Part E J Process Mech Eng 225 (2) (2011) 117–125.

[27] H. Zhai, Y. Dai, J. Wu, R. Wang, Energy and exergy analyses on a novel hybrid solar heating, cooling and power generation system for remote areas, Appl. Energy 86 (2009) 1395–1404.

[28] L. Jing, P. Gang, L. Yunzhu, W. Dongyue, J. Jie, Energetic and exergetic investigation of an organic Rankine cycle at different hot side temperatures, Energy 38 (2012) 85–95.